

# SIMULATIONS OF SURFACE EFFECTS AND ELECTRON EMISSION FROM DIAMOND-AMPLIFIER CATHODES\*

D. A. Dimitrov, R. Busby, D. Smithe, J. R. Cary, Tech-X Corp., Boulder, CO 80303, USA  
 I. Ben-Zvi, BNL, Upton, NY, USA and Stony Brook University, NY, USA  
 X. Chang, T. Rao, J. Smedley, Q. Wu, BNL, Upton, NY, USA  
 E. Wang, Peking University, Beijing 100081, China

## Abstract

Emission of electrons in diamond experiments based on the promising diamond-amplifier concept [1] was recently demonstrated [2]. Transmission mode experiments have shown the potential to realize over two orders of magnitude charge amplification. However, the recent emission experiments indicate that surface effects should be understood in detail to build cathodes with optimal properties. We have made progress in understanding secondary electron generation and charge transport in diamond with models we implemented in the VORPAL particle-in-cell computational framework. We introduce models that we have been implementing for surface effects (band bending and electron affinity), charge trapping, and electron emission from diamond. Then, we present results from 3D VORPAL diamond-vacuum simulations with the integrated capabilities on generating electrons and holes, initiated by energetic primary electrons, charge transport, and then emission of electrons from diamond into vacuum. Finally, we discuss simulation results on the dependence of the electron emission on diamond surface properties.

## INTRODUCTION

High-average current and high-brightness electron beams are needed in advanced applications such as ultra-high Free-Electron Lasers, electron cooling of hadron accelerators, and Energy-Recovery Linac light sources. To address the high requirements in these applications, a new design for a photoinjector with a diamond amplifier was proposed [1] and is currently being actively investigated [2, 3].

The new photoinjector concept has important advantages [1] (such as the ability to generate high-average current, high-brightness electron beams while providing a very long life time) compared to existing metallic and semiconductor photocathodes. The idea of its operation is to first generate a primary beam of electrons (accelerated to about 10 keV) using a conventional photocathode and inject them into diamond. The energetic primary electrons scatter inelastically in diamond, generating secondary electrons. These electrons, and their related holes, relax their energies initially by producing more electron-hole pairs.

\* The authors wish to acknowledge the support of the U.S. Department of Energy (DOE) under grants DE-SC0004431 (Tech-X Corp.), DE-AC02-98CH10886 (BNL), and DE-SC0005713 (Stony Brook University).

When the energy of these free charge carriers reaches close to the energy gap of diamond, further relaxation of their energy is dominated by scattering with phonons.

In applied electric field, the generated electron and hole clouds drift in opposite directions and are separated. The secondary electrons are transported towards a diamond surface with a negative electron affinity (NEA) used to improve emission. Over two orders of magnitude charge amplification (number of generated secondary electrons emitted relative to the number of primary electrons used as input) was already demonstrated [2, 4] experimentally.

Investigation of the phenomena involved in using diamond for generation of amplified electron beams via simulations requires modeling of secondary electron generation, charge transport, and electron emission. Here, we consider emission of electrons from diamond with both negative and positive electron affinity (PEA). Moreover, we implemented a model for band bending near the diamond emission surface and show that this effect leads to important changes in the electron energy distribution near the emission surface.

## SIMULATIONS

First, the simulations involve modeling generation of (secondary) electrons in the conduction band and holes in the valence band. These processes are initiated by inelastic scattering with highly energetic primary electrons injected into the diamond surface opposite to the emission one. The free electrons and holes relax their energies via inelastic scattering (creating more charge carriers and/or emission/absorption of phonons). The electrons drift (in applied field) towards the NEA surface. We have described in detail the models we implemented for secondary electron generation and charge transport in a previous study [5]. The final phase consists of modeling the effects near the diamond emission surface — propagation through the band bending region, reflection at the surface, and emission of electrons into vacuum. We implemented a simple emission model based on a stair-step surface potential:  $V(x, y, z) = 0$ , for  $x < 0$  and  $V(x, y, z) = \chi(y, z)$  for  $x > 0$ . The emission surface is at  $x = 0$  and  $\chi(y, z)$  is the electron affinity measured relative to the bottom of the conduction band at the surface. This is a starting choice to include the electron affinity in the emission since the resulting quantum mechanical problem can be solved analytically leading to expressions that are straightforward to evaluate. The prob-

ability for emission,  $P_e$ , for this model is given by

$$P_e = 4\sqrt{1 - \frac{\chi}{E \cos^2(\alpha)}} / \left(1 + \sqrt{1 - \frac{\chi}{E \cos^2(\alpha)}}\right)^2,$$

where  $E$  is the kinetic energy of a conduction band electron (also measured with respect to the same level as  $\chi$ ) and  $\alpha$  is the angle between the momentum of the electron and the normal to the diamond surface. This model allows studying both NEA and PEA effects. For NEA,  $P_e$  approaches unity quickly when  $E$  increases above zero and  $\alpha$  decreases below  $\pi/2$ . For PEA (e.g. of  $\chi = 0.5$  eV), there is a region of energies and angles for which electrons are only reflected.

The angle of refraction of the emitted electron is  $\sin \beta = \sqrt{E/(E - \chi)} \sin \alpha$  with  $\beta$  is also measured with respect to the normal to the surface. The amplitude of the emitted electron's momentum is given by  $\sqrt{2m_e(E - \chi)}$ .

We consider the band-bending region by introducing an additional field in the simulation confined within a region of the emission surface. The depth of this band bending region has been estimated from experiments [6] (and references therein) to be of the order of  $0.1 \mu\text{m}$  with the magnitude of the band bending approximately equal to  $0.36$  eV.

## RESULTS

We present results from VORPAL simulations on the effects of band bending and electron affinity on the energy distribution of electrons near the emission surface of diamond. The simulation domain has lengths of  $0.63 \times 3.67 \times 3.67 \mu\text{m}$  (with cell lengths of  $0.0124 \times 0.1183 \times 0.1183 \mu\text{m}$ ,  $51 \times 31 \times 31$  total number of cells) along the  $x$ ,  $y$ , and  $z$  axes, respectively. This domain consists of diamond with length (along  $x$ ) of  $0.6 \mu\text{m}$  followed by a vacuum region of  $0.03 \mu\text{m}$ . Following the approach in the diamond emission mode experiments [2], we set up the simulations to maintain a given potential difference along the ( $x$ ) length of the simulation domain using the feedback algorithm in VORPAL. We selected a potential difference such that the applied field in vacuum is  $5$  MV/m and in diamond is  $0.88$  MV/m (the dielectric constant of diamond is approximately  $5.7$ ).

The simulations proceed in 3 phases. First, we run for 6000 time steps to establish the desired potential difference across the diamond-vacuum simulation domain. We model diamond as a scalar dielectric using VORPAL's multi-field dielectric updater. In the second phase, we introduce a few (3 to 5)  $2.7$  keV primary electrons from the left boundary of the simulation domain (at  $x_{min}$ ) that start to produce secondary electrons and holes. This phase continues for about  $1$  ps leading to around 700 to 1000 total electrons. We use a time step of  $8.3 \times 10^{-17}$  s to resolve the impact ionization scattering rate in this phase.

Visualization of VORPAL particle data allows us to monitor the electron-hole generation processes (shown in the top two plots in Fig. 1 from a test simulation with primary electrons (yellow balls) entering into diamond from

the left side of the simulation box and initiating the creation of secondary electrons (blue) and holes (red)).

After secondary electron generation completes, we dump the simulation state and restore to execute the third, charge-transport, phase. This phase is dominated by electron-phonon and hole-phonon scattering. The first and third stages are run with a time step of  $3.7 \times 10^{-17}$  s. During the third phase, electrons drift (shown in the bottom left plot in Fig. 1) towards the vacuum region under the applied field while holes move to the opposite diamond surface and are extracted from the simulation when they cross it. When the electrons reach the emission surface of diamond, they are reflected or emitted into vacuum (a snapshot from the emission phase is shown in the bottom right plot in Fig. 1 with the electrons in vacuum colored in orange).

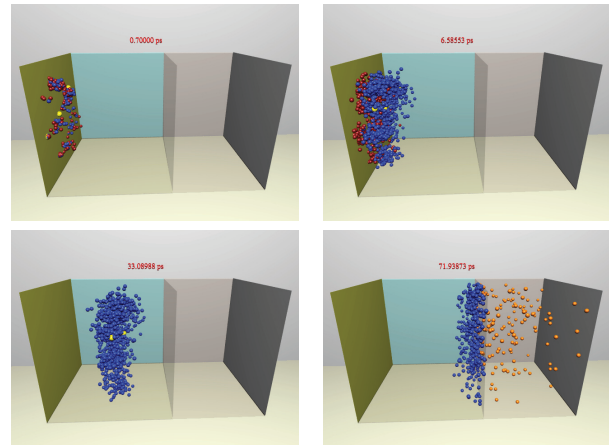


Figure 1: Visualization of electrons and holes at given times of a VORPAL simulation demonstrate primary electron injection, charge generation, and transport in diamond followed by electron emission in vacuum.

considered how electron affinity and band bending affect electrons near the diamond emission surface by measuring electron energy spread at different surfaces (with constant  $x$  values).

In Fig. 2, we plot energy histograms for one surface in diamond that is approximately one cell before the emission surface (left column of plots) and for the energies with which the electrons are emitted in vacuum (right column of plots).

Without band bending and with NEA of  $\chi = -0.1$  eV (top two plots), the electrons reach the diamond emission surface (top left plot) with average kinetic energy  $\langle E_k \rangle$  of  $0.12$  eV that is essentially equal to their  $\langle E_k \rangle$  in bulk diamond ( $0.11$  eV in these simulations). When emitted, their  $\langle E_k \rangle$  is  $0.23$  eV (top right plot). This increase is consistent with the  $\chi = -0.1$  eV NEA used. The two middle plots are from a simulation with the same parameters and in addition the band bending is turned on. The  $\langle E_k \rangle$  at the last cell before emission has now increased to  $0.27$  eV. Note that the max increase could be  $0.36$  eV but electrons also emit optical phonons while moving in the band bending region. After emission, their  $\langle E_k \rangle$  increases to  $0.41$  eV

which is somewhat higher than the magnitude of the NEA but within one standard deviation of it. Wang *et al.* [4] re-

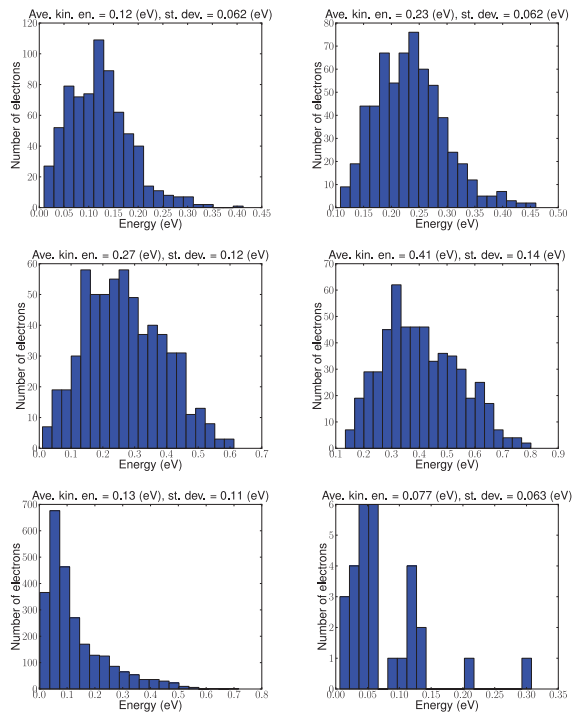


Figure 2: Energy distribution of electrons at two surfaces (see text) from three different simulation cases: (i) NEA of  $\chi = -0.1$  eV and no band bending (top row), (ii) same NEA and with band bending (middle row), and (iii) for PEA of  $\chi = 0.5$  eV and band bending (bottom row).

cently developed a model that provides an explanation for the time evolution of the emission gain and of the electric field in diamond. The standard deviation for the energy distribution of electrons in diamond close to the emission surface was considered a fitting parameter in their model. A value of  $0.12 \pm 0.01$  eV was obtained when the model was fitted to experimental data. This value is consistent with the standard deviation from our simulations (shown in the left middle plot) and is likely due to the band bending since the standard deviation in the simulations without band bending (top left plot) is approximately twice smaller.

Finally, we plot results from a simulation with band bending and PEA of  $\chi = 0.5$  eV (bottom row of plots). Note that there are many more electrons in the energy histogram that is one cell before the emission surface in diamond (bottom left). This is due to the high number of electrons that are frequently reflected at the emission surface. These electrons cross the VORPAL history surface diagnostic multiple times and are recorded every time they cross. Since they do not have sufficient energy to be emitted, they are trapped near the surface. Only a small number of electrons are emitted (bottom right plot) and their  $\langle E_k \rangle$  is now decreased to 0.077 eV. These results are consistent with the electron affinity and band bending values used.

## 05 Beam Dynamics and Electromagnetic Fields

### D06 Code Developments and Simulation Techniques

## SUMMARY

We reported here initial results from VORPAL simulations on electron emission from diamond. The simulations are based on algorithms we recently prototyped to model electron emission, band bending, negative and positive electron affinity. The results from these simulations confirm that it is of importance to include all of these effects when investigating electron emission from diamond.

Note, however, that the emission model we investigated is based on a simple stair-step potential does not take into account the effects of applied field and image charge. We are considering how to add such capabilities based on the Airy function approach for the calculation of the transmission probability [7] in a future development. Moreover, we are also investigating the addition of a thin triangular barrier to the potential to describe the dipole layer at the surface. Such a barrier was previously proposed by Orlov *et al.* [8] for emission from GaAs. They estimated the width of the activation (Cs,O) layer to be 0.7 nm with the height of the triangular barrier equal to the electron affinity of a clean GaAs surface.

In a future study, we will add modeling of surface roughness effects and how well results from simulations with the implemented models compare to available experimental data.

## REFERENCES

- [1] I. Ben-Zvi, X. Chang, P. D. Johnson, J. Kewisch, and T. Rao. Secondary emission enhanced photoinjector. C-AD Accelerator Physics Report C-A/AP/149, Brookhaven National Lab, 2004.
- [2] Xiangyun Chang, Qiong Wu, Ilan Ben-Zvi, Andrew Burrill, Jorg Kewisch, Triveni Rao, John Smedley, Erdong Wang, Erik M. Muller, Richard Busby, and Dimitre Dimitrov. Electron beam emission from a diamond-amplifier cathode. *Phys. Rev. Lett.*, 105(16):164801, Oct 2010.
- [3] J. D. Rameau, J. Smedley, E. M. Muller, T. E. Kidd, and P. D. Johnson. Properties of hydrogen terminated diamond as a photocathode. *Phys. Rev. Lett.*, 106(13):137602, Mar 2011.
- [4] E. Wang, I. Ben-Zvi, T. Rao, D. A. Dimitrov, X. Chang, Q. Wu, and T. Xin. Secondary-electron emission from hydrogen-terminated diamond: experiments and model. (*submitted*), 2011.
- [5] D. A. Dimitrov, R. Busby, J. R. Cary, I. Ben-Zvi, T. Rao, J. Smedley, X. Chang, J. W. Keister, Q. Wu, and E. Muller. Multiscale three-dimensional simulations of charge gain and transport in diamond. *J. Appl. Phys.*, 108(7):073712, 2010.
- [6] F. Maier, J. Ristein, and L. Ley. Electron affinity of plasma-hydrogenated and chemically oxidized diamond (100) Surface. *Phys. Rev. B*, 64:165411–1/7, 2001.
- [7] K. L. Jensen. On the application of quantum transport theory to electron sources. *Ultramicroscopy*, 95:29–48, 2003.
- [8] D. A. Orlov and V. E. Andreev. Elastic and Inelastic Tunneling of Photoelectrons from the Dimensional Quantization Band at  $p^+$ -GaAs-(Cs, O) Interface into Vacuum. *JETP Lett.*, 71:151–4, 2000.